



Engineered cementitious composite with characteristic of low drying shrinkage

Jun Zhang ^{a,b,*}, Chengxu Gong ^a, Zili Guo ^a, Minghua Zhang ^a

^a Department of Civil Engineering, Tsinghua University, Beijing, 100084, China

^b Key Laboratory of Structural Engineering and Vibration of China Education Ministry, Tsinghua University, Beijing, 100084, China

ARTICLE INFO

Article history:

Received 25 October 2007

Accepted 29 November 2008

Keywords:

Tensile properties

Shrinkage

Composite

Fiber reinforcement

ABSTRACT

This paper reports a new class of engineered cementitious composite (ECC) with characteristics of low drying shrinkage, tight crack opening and high tensile strain capacity. Research emphasis is placed on the influence of different cementitious matrix on drying shrinkage, tensile property and early age cracking behavior of the composites. Experimental results show that drying shrinkage of the composite is greatly reduced as using the low shrinkage cementitious material in matrix, while the composite remains strain-hardening and multiple cracking characteristics. The measured drying shrinkage strain at 28 days is only 109×10^{-6} to 242×10^{-6} for low shrinkage ECCs. For traditional ECC, the shrinkage strain at 28 days is nearly 1200×10^{-6} . The average tensile strain capacity after 28 days curing is 2.5% of the low shrinkage ECC with tensile strength of 4–5 MPa. Further, in the strain-hardening and multiple cracking stage, cracks with much smaller width compared to the traditional ECC are formed in the low shrinkage ECC.

© 2009 Elsevier Ltd. All rights reserved.

1. Introduction

Concrete is a typical brittle material that behaves as decaying load and immediate localizing the deformation at the location of first cracking after the peak load. Therefore, in normal concrete structures, as the stress exceeds the tensile strength of concrete, a single crack forms and the crack width quickly achieves a macro visible level in order to dissipating the large deformation requirement from both mechanical and environmental loads. Cracking in structures reduces the load-carrying capacity, and allows water and other chemical agents, such as deicing salt, to go through the cover layer to come into contact with the reinforcements, finally leads the structure failure due to the durability of concrete. Many methods have been proposed to improve the durability of concrete structures in the past, but, however few solutions have focus on that to overcome the brittle and tensile softening natures of concrete, which leads the formation of single crack with large opening. To effectively solve this serious problem, a fundamental solution reducing the brittle nature of concrete, especially reducing the crack width in concrete during its service stage must be found [1].

In recent years, a class of high performance fiber reinforced cementitious composite, called Engineered Cementitious Composites (ECC), which are defined by an ultimate strength higher than their first cracking strength and the formation of multiple cracking during the inelastic deformation process has been developed [2].

After first cracking, tensile load-carrying capacity continues to increase, resulting in strain-hardening accompanied by multiple cracking. The development of individual crack width can be described as that first increases steadily up a certain level, thereafter the crack width stabilizes and tends to remain constant. Further increasing in strain capacity is obtained by the formation of additional cracks until the material is saturated. After that, a single crack localizes and the load slowly drops with increased deformation. The spacing between multiple cracks in a typical ECC is about 3 to 6 mm, and the crack opening at the saturated stage is around 60 μm [2]. With this magnitude of crack width, the durability of material can be improved compared to the conventional concrete material with the similar deformation capacity.

However, in order to obtain this strain-hardening and multiple cracking behaviors, only a small amount of fine sand is allowed to be applied in the matrix in order to control fracture toughness of matrix [3–5]. Coarse aggregates are eliminated in the mixture also, resulting in higher cement content compared with conventional concrete. As a result of this special requirement, a high drying shrinkage strain must be developed during setting and hardening of the composite. For normal concrete, an ultimate drying shrinkage strain with magnitude of 400×10^{-6} to 600×10^{-6} will be produced under normal drying conditions of 20 °C and 60% relative humidity [6]. By contrast, the ultimate drying shrinkage strain of conventional ECC is approximately 1200×10^{-6} to 1800×10^{-6} under the similar drying conditions [7,8]. Due to this great difference in shrinkage deformation, more shrinkage induced cracking may happen as applying the ECC material in structures. These shrinkage cracks in structure may still lead long term durability problems even with small crack opening compared to the case without any cracks. Indeed, we always wish less cracks occur

* Corresponding author.

E-mail address: junz@tsinghua.edu.cn (J. Zhang).

Table 1

Chemical contents of the composite cement (%).

CaO	SiO ₂	Al ₂ O ₃	Fe ₂ O ₃	MgO	K ₂ O	Na ₂ O	TiO ₂	LOI
33.75	19.63	18.03	0.47	1.28	0.50	0.28	0.62	6.26

in structures. Desired situation should be the case there is no cracking also in the structure made of ECC as no cracking happens in the structure made of normal concrete under the similar environmental conditions. Therefore, developing new generation of ECC materials with drying shrinkage deformation comparable to normal concrete, but maintaining the excellent strain-hardening and multiple cracking performances becomes a new challenge to material designers and inventors.

In the present paper, a new class of ECC with characteristic of low drying shrinkage is present. The experimental results show that by applying the new type of cementitious matrix, the composite drying shrinkage can be greatly reduced. The drying shrinkage strain at 28 days is only 109×10^{-6} to 242×10^{-6} , while the average ultimate tensile strain is still able to achieve 2.5%. In addition, the crack width in the strain-hardening stage of the low shrinkage ECC is much smaller than that in traditional ECC. The new ECC can be characterized as low drying shrinkage, tight crack opening and high tensile strain capacity.

2. Experimental program

Three parts of investigation are involved in the experimental program. First, the influence of the type of cementitious matrix, as well as the mixture parameters, such as water to cementitious material ratio (w/c) and sand to cementitious material ratio (s/c), on drying shrinkage of the composite were experimentally quantified. Second, the influence of cementitious binder, as well as mixture parameters of w/c and s/c, on the composite tensile behavior was evaluated and compared between traditional and newly developed ECCs. Third, the influence of drying shrinkage deformation on early age cracking behavior of ECC under restrict condition was assessed. Three types of tests, drying shrinkage, uniaxial tension and two direction restricted plate drying tests were carried out in the experimental program.

2.1. Materials

In the present investigation, two types of cements, ordinary Portland cement used for traditional ECC matrix and the newly developed composite cement with low drying shrinkage characteristic used for new ECC matrix. The chemical content of the composite cement is listed in Table 1. Silica sand with average particle size 0.1 mm was used to form the matrix. Polyvinyl Alcohol fiber (PVA) supplied by Kuraray Company in Japan was employed as reinforcement and the fiber properties are listed in Table 2. Mixture proportions for low shrinkage ECC adopted in this study and for traditional ECC are given in Tables 3 and 4 respectively. For low shrinkage matrix, three different water to cementitious material ratio (w/c) of 0.45, 0.50, 0.55 and three different sand to cementitious material ratio (s/c) of 0.8, 1.1,

Table 2

Mix proportions of low shrinkage ECCs.

Mixture no.	Composite cement	Water	Sand	Super plasticizer	Fiber (vol.%)
1	1.0	0.45	0.8	0.012	1.7
2	1.0	0.45	1.1	0.018	1.7
3	1.0	0.45	1.4	0.022	1.7
4	1.0	0.50	0.8	0.011	1.7
5	1.0	0.50	1.1	0.013	1.7
6	1.0	0.50	1.4	0.020	1.7
7	1.0	0.55	0.8	0.010	1.7
8	1.0	0.55	1.1	0.011	1.7
9	1.0	0.55	1.4	0.016	1.7

Table 3

Parameters of the PVA fiber.

Density (g/cm ³)	Tensile strength (MPa)	E (GPa)	Diameter (mm)	Length (mm)
1.2	1620	42.8	0.039	12

1.4 were used to investigate the effect of w/c and s/c on material properties, including drying shrinkage deformation, tensile performance. In our tests, the workability for different mixture was adjusted by adding superplasticizer to maintain a similar fresh composite flowability.

2.2. Specimens, curing and testing procedures

For drying shrinkage test, a prism shape specimen measuring $40 \times 40 \times 160$ mm with two embedded copper heads at the two long ends for length measurement was used. After removing from their molds (24 h after casting), the specimens were stored in the room with constant temperature and relative humidity of 25 ± 2 °C and $60 \pm 1.5\%$ for drying shrinkage deformation measurement. The length measurement starts immediately after specimen demolding until 28 days after casting.

The uniaxial tensile tests give tensile stress-strain performance and related mechanical parameters, such as tensile strength and strain of materials. Rectangular coupon specimens with size of $40 \times 160 \times 15$ mm were used to conduct uniaxial tensile test for each mixture at age of 3, 7 and 28 days. The molds used to cast the tensile specimens were made of steel. After removing from their molds, the tensile specimens were stored in water at 20 ± 2 °C for curing until tensile tests were carried out. The tensile specimens were tested in uniaxial tension with displacement control in a 250 kN capacity MTS 810 material testing system with hydraulic wedge grips. Aluminum plates were epoxy glued onto the ends of the specimens prior to loading at least 6 h to enhance the ends for gripping. The actuator displacement rate used for controlling the test was 0.0025 mm/s. The strain was measured by two extensometers mounted on the surface of the specimen. The measured gage length of extensometer was 50 mm. The tensile test set-up and specimen with aluminum plates glued and extensometers mounted is shown in Fig. 1. The raw data consisted of time, load, position of the piston and displacement from each extensometer. The tensile behavior can then be determined from these test data.

To evaluate the influence of drying shrinkage deformation on early age cracking behavior of new developed and traditional ECCs, two direction restricted plate tests were conducted also in the present study. A square plate with dimension of $600 \times 600 \times 63$ mm was used in the test. The restriction to the plate specimen is provided by two layers of steel bolts with 100 mm in length and 8 mm in diameter, one end fixed with the boundary steel beam and the other end exposed inside the casting mold. A total of 56 steel bolts were used along the four boundary beams. After casting material into the mold, the dimension of the plate can then be regarded as approximately fixed without length changing. Thus shrinkage induced cracking should occur immediately as long as the shrinkage deformation developed in the composite is sufficiently large and the restricted action provided by the steel bolts is effective. The mold before material casting is shown in Fig. 2. The test was carried out in a room with temperature and relative humidity of 25 ± 5 °C and 40%–60%. After specimen casting, the plate surface were covered with plastic sheet for one day

Table 4

Mix proportion of traditional ECC.

Mixture no.	Portland cement	Fly ash	Water	Sand	Fiber (vol.%)
10	1.0	0.25	0.5	0.8	1.7

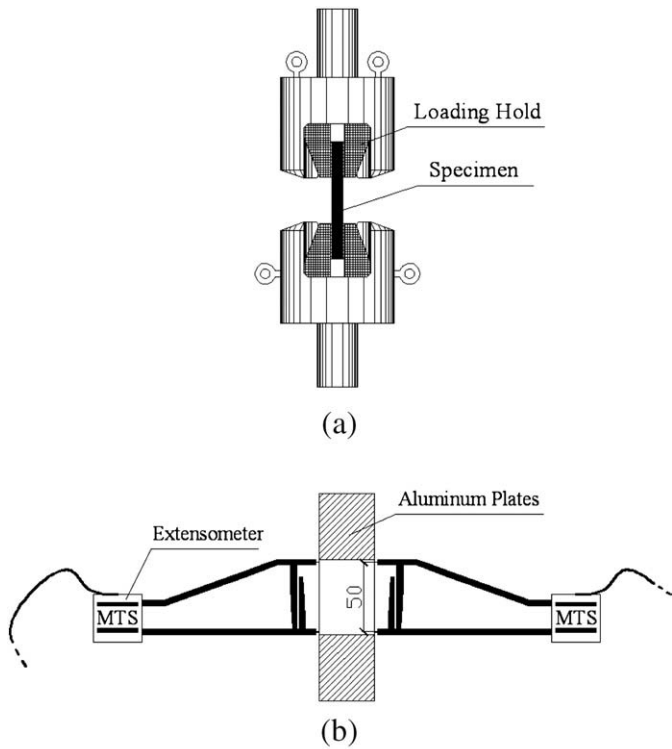


Fig. 1. Tensile test set-up (a) and specimen with aluminum plates glued and extensometers mounted.

before starting fast drying process. After one day curing, an electronic fan with constant wind velocity of 6 m/s was used to blow the plate top surface until 5 days since casting. By viewing the cracking patterns occurring on the top surface of the plate specimen, the effect of early age shrinkage of composite on cracking behavior under restrict condition can be assessed.

The mixing procedure of the composite material consists of the following steps. (1) Matrix preparation: The matrix was prepared in a mortar mixer. First, the cementitious material and silica sand were mixed together for 2 min at low speed. Then water with superplasticizer and viscous agent (methyl cellulose) mixed in were gradually added, and mixing was continued for 2 min which results in a uniform fluid matrix. Within this period, the bottom of the mixing bowl should be scraped manually to ensure that no solid materials stick to the bottom. After such scraping, the matrix was mixed at a higher speed for 1 min before addition of fibers. (2) Addition of fibers:



Fig. 2. Set-up of two-way restricted plate test.

the fibers were gradually spread into the mixer by hand as the matrix was mixed at a slow speed. The fibers must be added slowly to ensure proper distribution with no fibers bundled together. (3) Casting and curing: The composite material was carefully cast into the mold in two layers. First about half the material was placed. Then the mix was vibrated for about 1–2 min to ensure that the material was well compacted. Next, the second half of the mold was filled by the composite in the same manner. After smoothing the surface, the specimens were covered with a polyethylene sheet to prevent loss of moisture and stored for 24 h at room temperature prior to demolding or testing.

3. Results and discussions

3.1. Dry shrinkage of different ECC proportions

The measured drying shrinkage up to 28 days of different ECC mixtures in terms of strain-time diagrams is shown in Fig. 3, where no. 1 to no. 9 were made by low shrinkage cementitious material and no.10 was traditional ECC mixture using normal Portland cement in matrix. We can clearly see that the drying shrinkage deformation of the composites using the new cementitious material in matrix is greatly reduced. The shrinkage strain at 28 days is only 109×10^{-6} to 242×10^{-6} of the new developed ECCs. For traditional ECC, the shrinkage strain at 28 days is nearly 1200×10^{-6} that is almost 7 times larger than the shrinkage of low shrinkage ECCs. Further, the result indicates that the drying shrinkage of the ECCs with low shrinkage cementitious matrix is even lower than that of normal concrete, which normally has the magnitude of shrinkage strain of $400 \sim 600 \times 10^{-6}$ at 28 days under the similar testing conditions. This means that under the same or similar curing periods and environmental conditions, as cracking does not occur in normal concrete structure, the same or even higher no-cracking guarantee can be provided as using the new ECC to replace normal concrete in the structure.

For the low shrinkage ECC, the effects of water to cementitious material ratio (*w/c*) and sand to cementitious material ratio (*s/c*) on the drying shrinkage behavior were investigated also by varying the two parameters in the mix proportions. Figs. 4 and 5 display the shrinkage strain versus time diagrams of the composites having different *w/c* (0.45, 0.50, 0.55) and *s/c* (0.8, 1.1, 1.4). From the results,

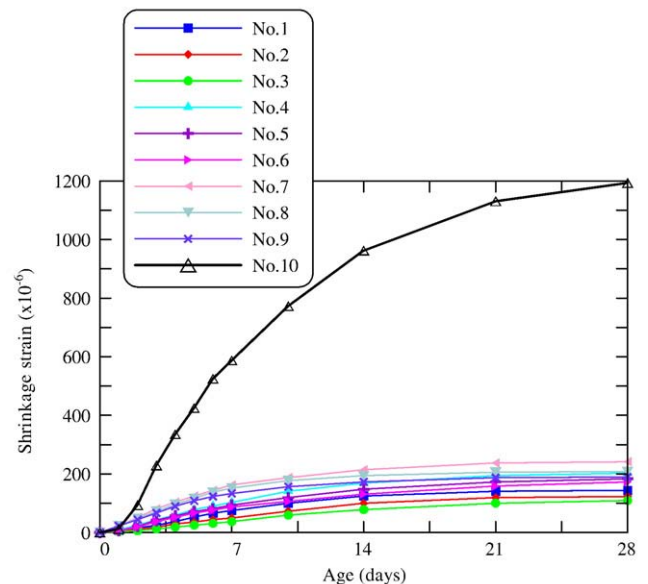


Fig. 3. Development of dry shrinkage strain with curing time of different ECCs.

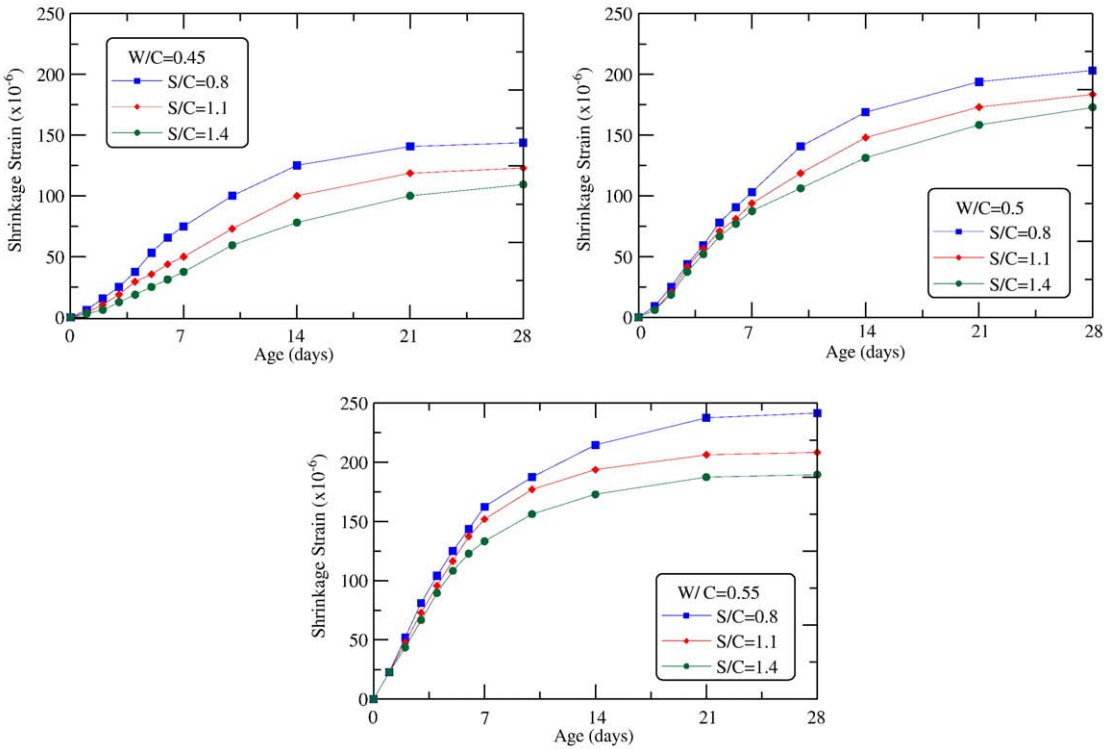


Fig. 4. Effect of s/c on dry shrinkage of ECCs with different w/c.

first we can see that for a given age, the drying shrinkage deformation reduces with decrease of w/c. For instance, as s/c is equal to 0.8, the shrinkage strain of the composite at 28 days is 144, 203 and 242 microstrains respectively for w/c is equal to 0.45, 0.50 and 0.55

respectively. Second, the shrinkage strain reduces with increase of s/c. The more the fine aggregate, the less the shrinkage deformation of the composite. The above influencing law of w/c and s/c on drying shrinkage of ECC is consistent with that found in normal concrete [6].

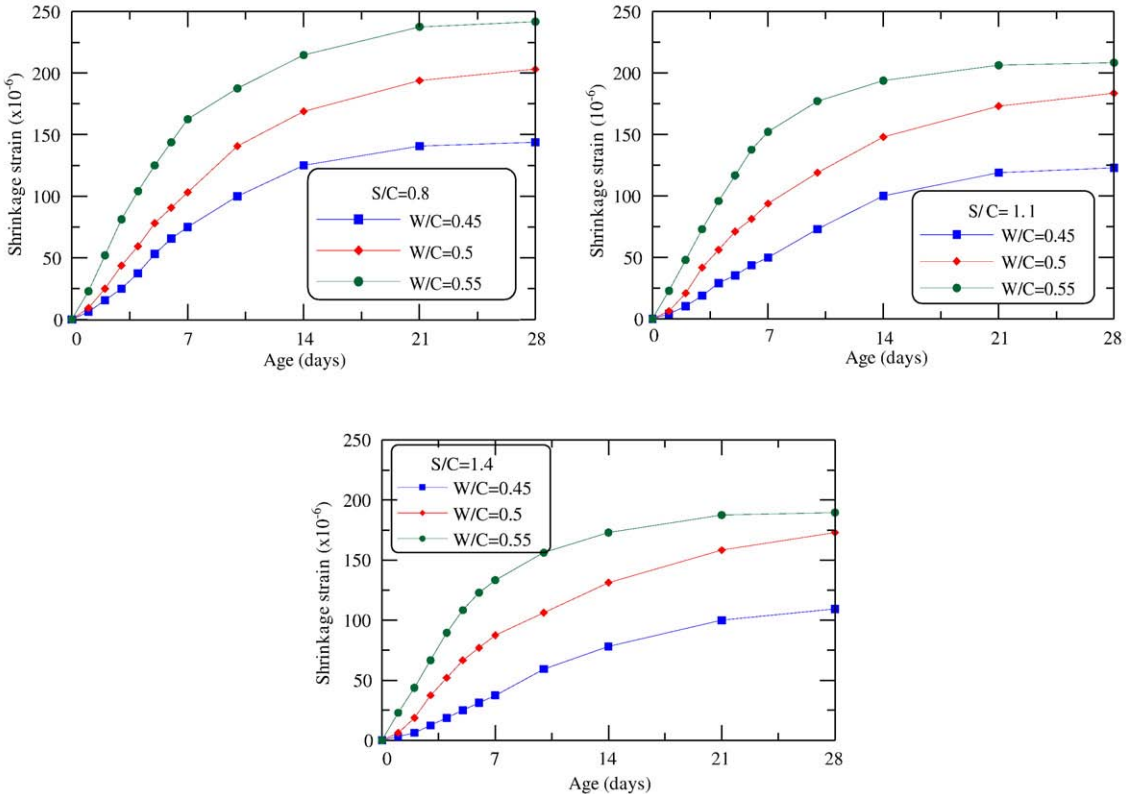


Fig. 5. Effect of w/c on dry shrinkage of ECCs with different s/c.

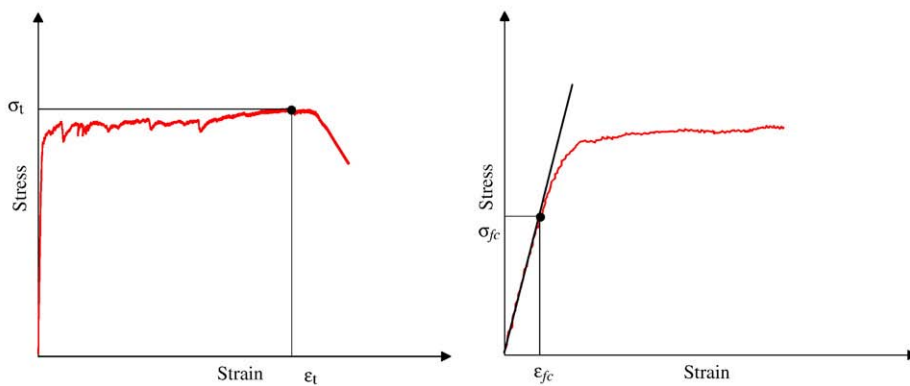


Fig. 6. Definition of some tensile parameters.

Less water content will lead to less water lost during drying. More aggregates will lead to more restraints to cement paste shrinkage. However, higher s/c will result in worse effect on tensile performance. In current study, the variation range of drying shrinkage strain is between 109×10^{-6} to 242×10^{-6} as w/c varying from 0.45 to 0.55 and s/c varying from 0.80 to 1.40. The maximum and minimum shrinkage strains listed above are corresponding to w/c = 0.55, s/c = 0.8 and w/c = 0.45, s/c = 1.4. Certainly, we need to note that the drying shrinkage is not the only concerned property to evaluate the overall performance of the composite. The other mechanical properties, in particular tensile behavior is also critical to achieve the target of the present work.

3.2. Uniaxial tensile behavior of different ECC proportions

To analyze the tensile results, first we define some mechanical parameters based on experimentally determined uniaxial tensile stress-strain diagram. Fig. 6 shows a typical measured tensile stress-strain curve. The curve can be divided into three sections: (1) elastic stage up to first cracking occurs: the point of first cracking is corresponding to the end of the initial linear section of the stress-strain curve, the corresponded stress is known as cracking strength σ_{fc} , and the corresponded strain is called first cracking strain ε_{fc} ; (2) strain hardening stage: tensile load-carrying capacity continues to increase, resulting in strain-hardening accompanied by multiple cracking, the maximum stress is the tensile strength σ_t and the corresponded strain is ultimate tensile strain ε_t ; (3) strain softening stage: a single crack localizes and the load slowly drops with increased deformation. Base on tensile test results, the corresponded first cracking strength and strain, the ultimate tensile strength and strain of each ECC mixture shown in Tables 1 and 3 are listed in Tables 5–7 for three typical ages of 3, 7 and 28 days respectively. To compare the tensile performance of the new and traditional ECCs, the tensile stress-strain diagrams of the traditional ECC (no. 10) and the low shrinkage ECC (no. 7) at different curing period of 3, 7 and 28 days are shown in Fig. 7(a) to (e). To

investigate the cracking pattern and crack width under tensile loading, Fig. 8(a) and (b) displays typical stress-strain curve of mix no. 7 and mix no. 10 respectively along with specimen photographs taken under different loading stages. Fig. 9(a) and (b) presents the enlarged photographs of the crack patterns under loading of the two mixtures at typical strain levels of 1.0% and 1.7%. To compare the cracking patterns of the two mixes, the specimens with different curing age, but having similar stress-strain curve were selected.

From these experimental results, first we can see that after using the low shrinkage cementitious material as binder, the composite is not only able to remain the strain-hardening and multiple cracking performances, but also able to achieve a high ultimate tensile strain capacity. At the moment of drying shrinkage greatly reduced, the new developed ECC (no. 7) material has even higher ultimate tensile strain capacity than that of traditional ECC (no. 10). The average ultimate tensile strain at 3, 7 and 28 days after casting is 2.77%, 2.46%, 2.61% and 0.51%, 1.52%, 0.80% for new and traditional ECCs respectively. Second, in the strain-hardening stage, smoother stress-strain diagram is obtained from the new ECC specimens compared with that of the traditional ECC. The smooth stress-strain curve means that the stress jump during crack formation is small. The load can stably be

Table 6
Tensile properties of different ECCs (7 days).

Mixture no.	ε_{fc} (%)	σ_{fc} (MPa)	ε_t (%)	σ_t (MPa)
1	0.015	2.173	0.740	4.592
2	0.015	1.768	0.865	3.819
3	0.014	2.336	0.532	4.245
4	0.020	2.160	0.820	4.147
5	0.017	2.200	0.292	3.897
6	0.015	1.756	0.786	3.697
7	0.021	1.913	1.987	3.874
8	0.021	2.135	0.966	3.783
9	0.023	2.334	0.558	3.442
10	0.018	2.630	1.363	4.390

Table 5
Tensile properties of different ECCs (3 days).

Mixture no.	ε_{fc} (%)	σ_{fc} (MPa)	ε_t (%)	σ_t (MPa)
1	0.015	1.687	1.741	2.921
2	0.015	1.470	0.574	2.195
3	0.013	1.228	0.833	1.951
4	0.014	0.730	0.956	2.104
5	0.020	1.818	0.369	3.571
6	0.016	2.298	0.275	3.572
7	0.019	1.807	2.772	3.801
8	0.026	2.203	1.096	3.386
9	0.024	1.698	0.980	3.578
10	0.023	1.674	0.741	3.373

Table 7
Tensile properties of different ECCs (28 days).

Mixture no.	ε_{fc} (%)	σ_{fc} (MPa)	ε_t (%)	σ_t (MPa)
1	0.022	2.696	1.493	4.841
2	0.020	2.562	0.552	3.849
3	0.019	3.102	0.759	4.049
4	0.027	2.674	1.236	4.032
5	0.024	2.988	0.387	3.874
6	0.018	2.779	0.531	4.072
7	0.028	2.605	2.608	4.303
8	0.027	2.655	1.146	3.983
9	0.021	2.621	0.496	3.883
10	0.014	2.931	0.837	4.777

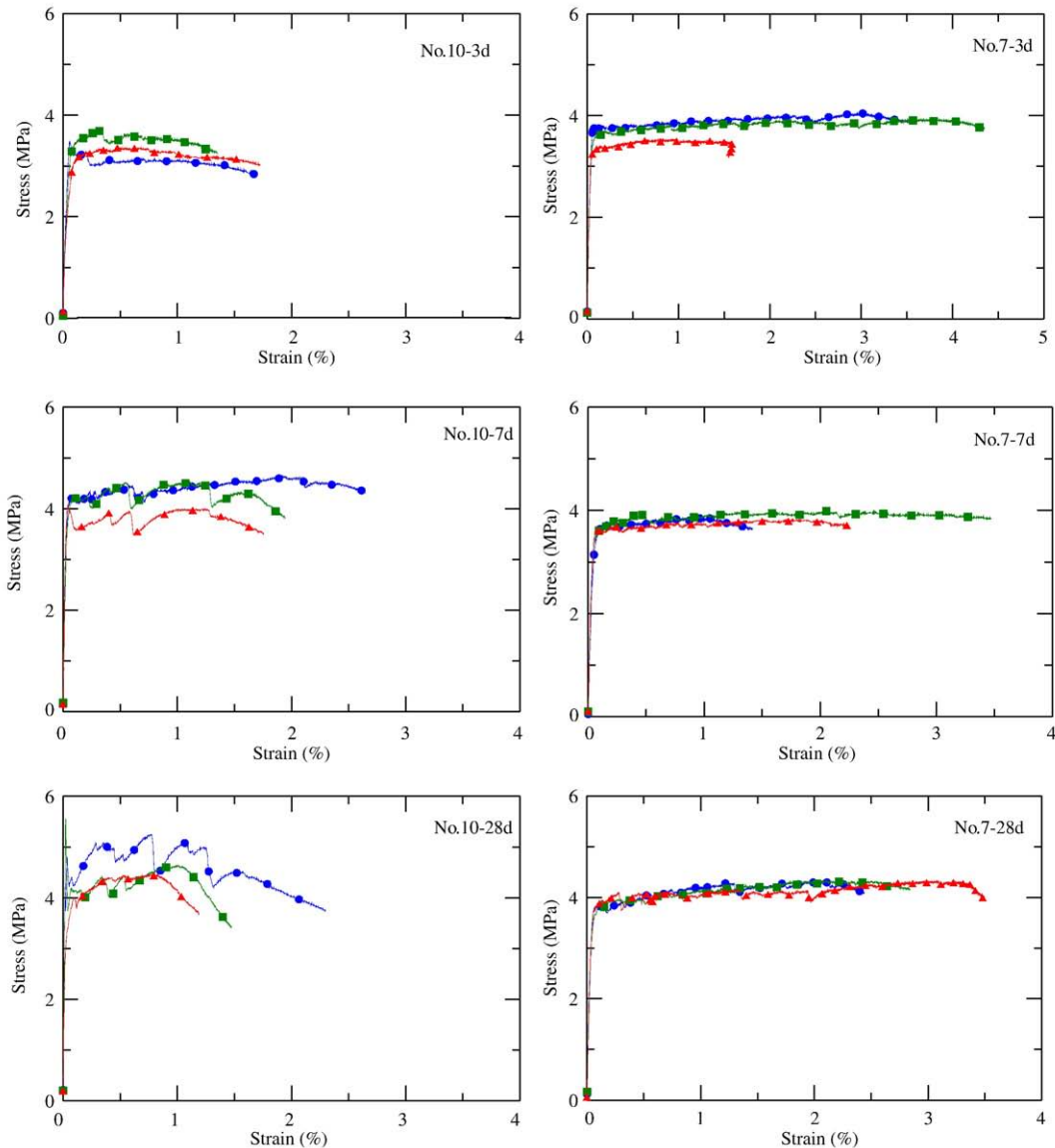


Fig. 7. Stress strain diagrams of mixtures no.7 and no.10 at different ages.

transferred by the fibers crossing the cracks. In contrast, the stress jump is obvious in the traditional ECC during the formation of cracks except for the results of 3 days, that has a similar behavior as low shrinkage ECC has. The reason for above exception may be due to the low fiber-matrix bond strength at early age and leads a similar fiber bridging behavior as that of low shrinkage ECC. Third, finer cracks are formed in the new ECC within strain-hardening stage. This interesting finding can easily be validated by viewing the photographs of the specimen under different loading points, see Figs. 8 and 9. The pictures clearly show that for the low shrinkage ECC (no. 7), almost no visible crack can be seen even though the specimen is stressed in tension at high strain level, such as 1.0% and 1.7%. In contrast, much more visible cracks can be observed on the conventional ECC specimen (no. 10) at the strain level of 1.0% and 1.7%. Based on this simple observation, we may believe that the crack width under the same tensile strain level of the two composites is obviously different. Cracks with much smaller width are formed in the low shrinkage ECC can be concluded. This finding suggests that low shrinkage ECC will most likely have lower permeability and better durability even in presence of micro cracks when compared with cracked concrete in

which the crack width is usually in the range of several hundred micron meters to several millimeters due to without crack width controlling function. The formation of very fine crack may also be responsible to the smoother stress-strain diagram.

A possible mechanism that contributes to the improvements on mechanical and cracking performances of the new developed ECC may be that the lower matrix shrinkage reduces the bond strength of fiber and matrix [9]. High bond strength will lead to more fiber rupture during fiber pullout from matrix microscopically and result in worse strain-hardening and multiple cracking performances macroscopically [10–12]. As the drying shrinkage of matrix decreases, the clamping pressure acting on the fiber surface, which mostly results from shrinking of surrounding matrix, should decrease also and this leads a reduction of the fiber-matrix bond strength. To evaluate the influence of material shrinkage on fiber-matrix interfacial bond properties, bond strength in particular, a simple model developed by Stang [9] is used to calculate the clamping pressure and the frictional based shear strength of PVA fiber and cement matrix. In the model, assuming a Coulomb type of friction on the debonding interface of fiber and matrix, the relationship between clamping pressure stress

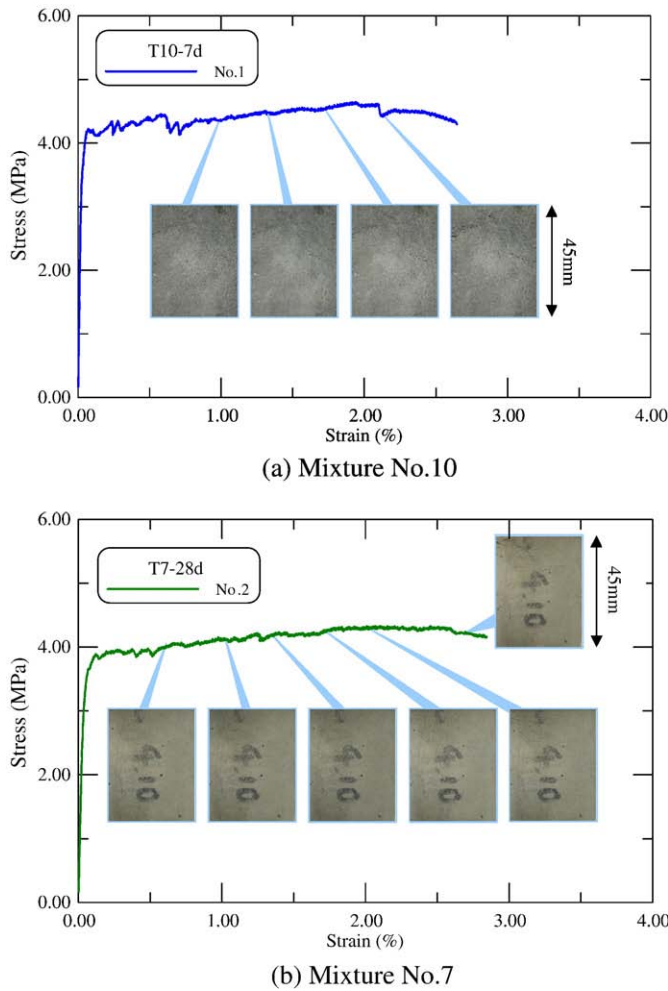


Fig. 8. Typical stress–strain curves of mix no.10 (a) and mix no.7 (b) shown along with specimen photographs taken under different loading stages.

(p) acting on the fiber/matrix interface and fiber/matrix frictional shear strength can be expressed as

$$\tau = \mu p \quad (1)$$

Where μ is the coefficient of friction. The clamping pressure stress can be related with composite shrinkage strain (ε_{sh}) by [9]

$$p = \frac{E_m \varepsilon_{sh}}{\frac{1 + v_m}{1 + v_f} + \frac{E_m}{E_f} (1 - 2v_i)} \quad (2)$$

Here E_m , v_m and E_m , v_m are elastic modulus and Poisson's ratio of matrix and fiber respectively. Replace p in Eq. (1) with Eq. (2), we obtain the correlation between frictional shear strength and composite shrinkage strain as

$$\tau = \frac{\mu E_m}{\frac{1 + v_m}{1 + v_f} + \frac{E_m}{E_f} (1 - 2v_f)} \varepsilon_{sh} \quad (3)$$

Thus, the influence of composite shrinkage deformation on clamping pressure stress p and shear bond strength τ can be assessed by Eqs. (2) and (3). In Table 8, the elastic constants for PVA fiber and cement matrix used in clamping pressure and frictional shear strength calculations are shown together with assumed value of coefficient of friction, where the related parameters of the two additional traditional ECC mixtures from references [8,13] are listed also for comparison. The difference in shrinkage strain of the two additional

ECC mixtures results from the difference of fly ash content [8]. Regarding the coefficient of friction of PVA fiber and cement matrix, no direct measurements can be found in literature. However, the coefficient of friction between carbon fiber, polypropylene fiber and cement matrix reported by Stang [9] should be in the range of 0.05 to 0.1 and 0.3 to 0.5 respectively. Considering the PVA fiber is harder than polypropylene fiber and softer than carbon fiber, we assume the coefficient of friction between PVA fiber and cement matrix to be in the range of 0.15 to 0.25. In Table 8, the predicted clamping pressure at typical ages since composite casting along with predicted Coulomb frictional bond strength of PVA fiber and cement matrix during fiber pullout of the typical low shrinkage ECC (no. 7) and three traditional ECCs listed in Table 8 are shown together with some experimental determined frictional bond strengths in traditional ECCs reported in the literatures [13]. From the theoretical results listed in Table 9, first we can find that the calculated range of values for the frictional bond strength correspond extremely well to corresponding values from experiments by fiber pullout test [13]. Therefore, we may conclude that the given value of coefficient of friction between PVA fiber and cement matrix is reasonable for bond strength analysis. Second, the calculated results clearly show that the reduction of matrix shrinkage deformation can extraordinarily lower the clamping pressure and leads remarkable reduction in bond strength of fiber and matrix. The bond strength of fiber and matrix in traditional ECC (no. 10) is almost 10 times higher than that of low shrinkage ECC (no. 7). The advantages of lowering the bond strength may include two aspects. First the reduction of interface bond strength leads to less fiber rupture. Second, as interface bond decreases, the fiber pullout length from matrix will increase that in turn enhances the fiber bridging behavior and leads composite tensile performance improved. For a fiber with

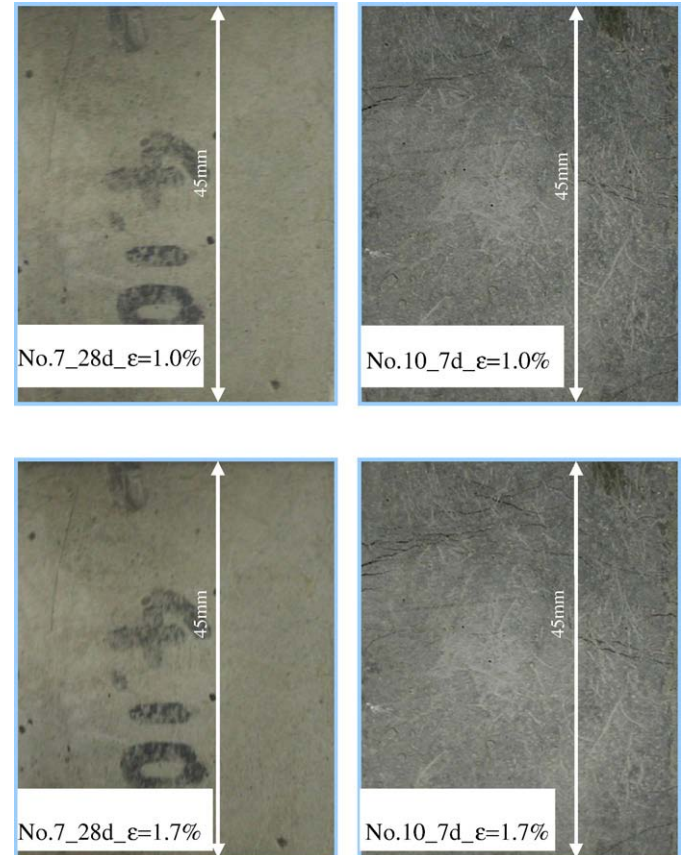


Fig. 9. Enlarged photographs of crack patterns under loading of the two mixtures at typical strain levels of 1.0% and 1.7%.

Table 8

Elastic constants, shrinkage strain and frictional coefficient of PVA fiber–matrix interface.

Mix no. (time)	E_m (GPa)	ν_m	E_f (GPa)	ν_f	$\varepsilon_{sh} (\times 10^{-6})$	μ
7 (3 days)	7.4	0.2	42.8	0.3	81	0.15–0.25
7 (7 days)	9.9	0.2	42.8	0.3	163	0.15–0.25
7 (28 days)	11.2	0.2	42.8	0.3	242	0.15–0.25
10 (3 days)	7.4	0.2	42.8	0.3	229	0.15–0.25
10 (7 days)	17.3	0.2	42.8	0.3	588	0.15–0.25
10 (28 days)	23.3	0.2	42.8	0.3	1194	0.15–0.25
Ref_1 [13]	15	0.2	42.8	0.3	1800	0.15–0.25
Ref_2 [13]	15	0.2	42.8	0.3	1200	0.15–0.25

one end embedded in the matrix, the maximum embedment length L_c (fiber pullout length) that allows fiber to complete debonding without rupture can be calculated as [14]

$$L_c = \frac{\sigma_f d_f - \sqrt{8G_d E_f d_f}}{4\tau} \quad (4)$$

where σ_f , d_f and E_f are fiber strength, equivalent diameter and elastic modulus. τ and G_d are frictional and chemical bond strength of fiber and matrix respectively. Clearly, any reduction in either chemical bond G_d or frictional shear strength τ allows more fibers to enter the pullout stage, which is critical for increasing L_c and hence improving strain-hardening potential. In low shrinkage ECC, L_c may become 10 times longer even with assumption that the matrix shrinkage decrease does not influence the value of chemical bond strength G_d . Certainly, the bond strength is not the only parameter controlling the overall tensile performance of the composite. That is why the tensile performance of the rest mixtures except no. 7 of the low shrinkage ECC is not good as no. 7 presented although their bond strengths all are similar due to the close values of drying shrinkage strain and elastic constants. The ratio of w/c and s/c plays an important role also in overall tensile performance control.

The effect of w/c and s/c on composite tensile behavior of the low shrinkage ECC is investigated by varying the two parameters in the mix proportions. The experimentally determined σ_{fc} , ε_{fc} , σ_t and ε_t of different mixtures are listed in Tables 4–6. Fig. 10(a) and (b) plots the diagram of ultimate tensile strain versus s/c ($s/c = 0.8, 1.1, 1.4$) for the specimens undergo 7 and 28 days curing respectively. The effect of w/c on ultimate tensile strain is shown also in the figures by using different marks and colors in the figure. From the results, first we can observe that in the range of current tests, the lower the s/c, the higher the ultimate tensile strain. This effect is more pronounced as w/c = 0.55 and behaves a nonlinear way. For $s/c = 1.1$ to 1.4, the effect of s/c on ultimate tensile strain is not obvious. In the current study, the mixture with w/c = 0.55 and s/c = 0.8 has the highest ultimate tensile strain at 28 days of 2.61%. The mixture with w/c = 0.55 and s/c = 1.4 has the lowest ultimate tensile strain at 28 days of 0.4%. Previous experimental studies had also shown that less sand or smaller particle sand and higher w/c ratio in ECC will lead improvement of strain-hardening and multiple cracking performances of composite [15]. The mechanisms of high w/c and less s/c on tensile strain capacity

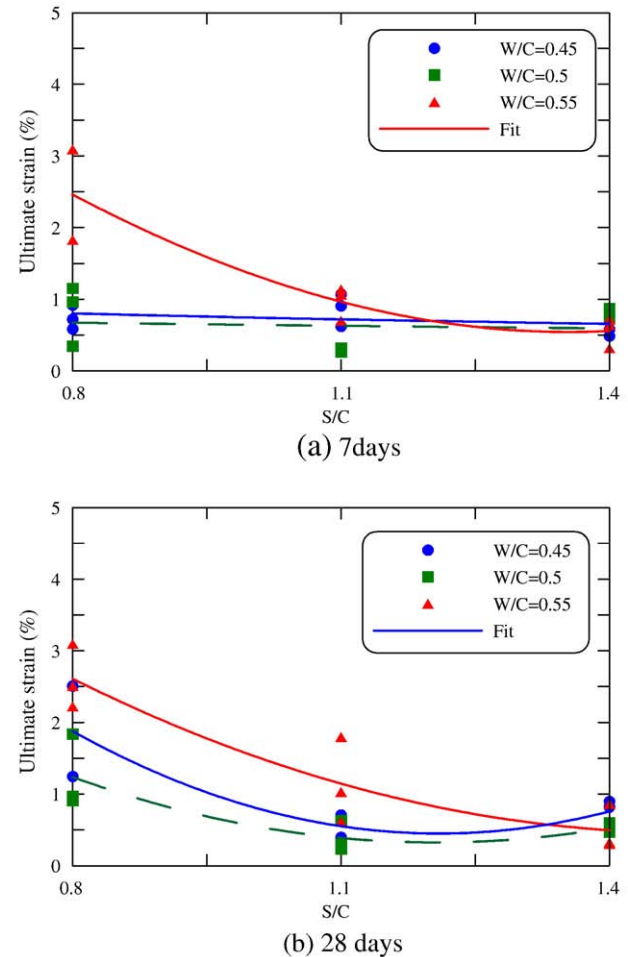


Fig. 10. Effect of s/c and w/c on ultimate tensile strain, (a) 7 days curing and (b) 28 days curing.

improvement may include both of lowering fracture toughness of matrix and improvement on fiber dispersion which in turn enhance the fiber bridging stress across a crack. Particular investigations on above aspects are needed. In addition, high content of sand may lead worse fiber bridging because fibers can not go through sand particles, which normally is larger than cement particles in the view of particle size, even though more sand will decrease drying shrinkage of the composite. Therefore, overall performance optimization needs taking all the concerned properties into account to avoid attending one and losing another.

The effect of w/c on tensile strength obeys the well-known law that lower w/c leads to high strength. The increase of s/c results in a little bit decrease of tensile strength. But the effect is limited within the variation range of the present study. As w/c and s/c are varied within 0.45 to 0.55 and 0.8 to 1.4 respectively, the tensile strength of 28 days curing is changed between 4 and 5 MPa. However, ultimate tensile strain is varied from 0.4 to 2.6%, which is sufficient large compared with tensile strength. The influence of w/c and s/c on the cracking strength is not obvious. The variation of cracking strength in all mixtures is within the range of 2.5–3.0 MPa after 28 days curing.

3.3. Cracking behavior of restricted plate specimen under fast drying process

The restricted plate test was conducted with low shrinkage ECC (no.7) and traditional ECC (no.10) respectively to reveal the effect of drying shrinkage deformation on early age cracking behavior of the composites. Fig. 11 displays the photographs of the two plates after

Table 9

Predicted clamping pressure and frictional bond strength of typical ECCs.

Mixture no. (time)	p (MPa)	$\tau_{Cal.}$ (MPa)	τ_{Test} (MPa)
7 (3 days)	0.80	0.12–0.20	–
7 (7 days)	1.50	0.23–0.38	–
7 (28 days)	2.62	0.40–0.66	–
10 (3 days)	1.72	0.26–0.43	–
10 (7 days)	9.37	1.41–2.34	–
10 (28 days)	24.38	3.66–6.10	–
Ref_1 [13]	25.39	3.81–6.35	3.5–6.5
Ref_2 [13]	16.93	2.54–4.23	1.9–4.2

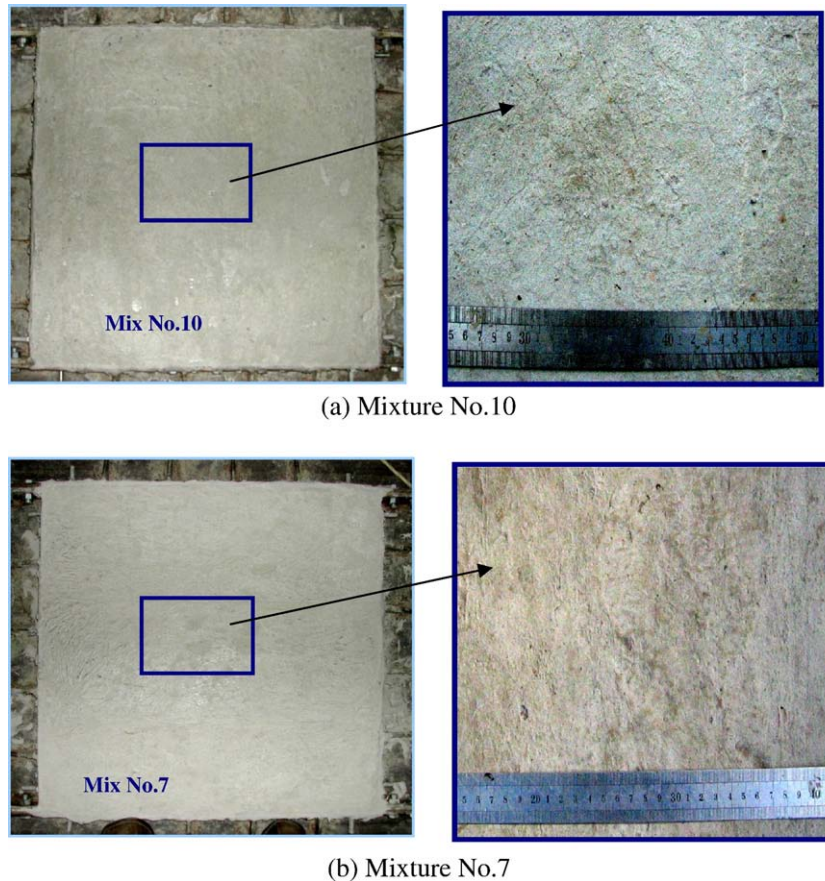


Fig. 11. Photographs of the two direction restricted plate specimens after undergoing fast drying process, (a) mix no.10 and (b) mix no.7.

undergoing fast drying process (4 days surface blowing under constant velocity of 6 m/s with an electronic fan), where one window shows full size of the specimen and the other enlarged window shows the small portion of the plate surface. By viewing the photographs, we can clearly see that there are a number of fine cracks on the surface of the plate made with conventional ECC mixture (no.10). The cracks almost grow along 45° to plate length direction due to the two-way restrictions provided by the 56 steel bolts (see Fig. 2). By contrast, no visible cracks can be found on the surface of the plate made with low shrinkage ECC (no.7). The interesting experimental results show that the effectiveness of reducing drying shrinkage on overcoming shrinkage induced early age cracking in structures is quite significant. Indeed, under the same restraint and fast drying conditions, cracking can never be prevented at all for normal concrete plate. This apparent improvement on early age shrinkage cracking control of the low shrinkage ECC must benefit the long-term durability of the ECC structures.

4. Conclusions

A new class of engineered cementitious composite with special focus on drying shrinkage reduction is developed. The measured drying shrinkage strain at 28 days is only 109×10^{-6} to 242×10^{-6} for low shrinkage ECCs. For traditional ECC (using normal Portland cement in matrix), the shrinkage strain at 28 days is nearly 1200×10^{-6} that is almost 7 times larger than the shrinkage of the composite with low shrinkage matrix. The developed new composite is not only able to reduce the drying shrinkage deformation remarkably, but also is able to remain the unique strain-hardening and multiple cracking performances. The composite demonstrated a tensile strain capacity around 2.5% and tensile strength 4–5 MPa while drying shrinkage

performance was significantly improved. In addition, the individual crack width in strain-hardening stage of the low shrinkage ECC is much smaller than that occurred in traditional ECC under the same tensile strain level. Restraint plate test demonstrates that the low shrinkage ECC behaves a better performance in prevention of early age shrinkage induced cracking. The developed ECC can be characterized as low drying shrinkage, tight crack opening and high tensile strain capacity. Above new features may significantly benefit the long-term durability of ECC structures.

Acknowledgments

Support from the National Natural Science Foundation of China (No. 50878119) is gratefully acknowledged.

References

- [1] J. Zhang, V.C. Li, S.N. Andrzej, S. Wang, Introducing ductile strip for durability enhancement of concrete slabs, *Journal of Materials in Civil Engineering* 14 (3) (2002) 253–261.
- [2] V.C. Li, Advances in ECC Research, *ACI Special Publication on Concrete: Material Science to Applications*, SP 206-23, pp. 373–400, 2002.
- [3] V.C. Li, From micromechanics to structural engineering—the design of cementitious composites for civil engineering applications, *JSCE J. of Struc. Mechanics and Earthquake Engineering* 10 (2) (1993) 37–48.
- [4] V.C. Li, D.K. Mishra, H.C. Wu, Matrix design for pseudo strain-hardening fiber reinforced cementitious composites, *Materials and Structures* 28 (183) (1995) 586–595.
- [5] J. Zhang, B. Leng, The transition from macro-multiple cracking to micro-multiple cracking in cementitious composites, *Tsinghua Science and Technology* 13 (5) (2008) 669–673.
- [6] A.M. Neville, *Properties of Concrete*, 3rd Edition Pitman Publishing Limited, 1981.
- [7] M. Li, V.C. Li, Behavior of ECC/concrete layer repair system under drying shrinkage conditions, *Proceedings of ConMat'05*, Vancouver, Canada, August, pp.22–24, 2005.

- [8] E.H. Yang, Y. Yang, V.C. Li, Use of high volumes of fly ash to improve ECC mechanical properties and material greenness, *ACI Materials Journal* 104 (6) (2007) 303–311.
- [9] H. Stang, Significance of shrinkage-induced clamping pressure in fiber-matrix bonding in cementitious composite materials, *Advanced Cement Based Materials* 4 (3–4) (1996) 106–115.
- [10] Z. Lin, V.C. Li, Crack bridging in fiber reinforced cementitious composites with slip-hardening interfaces, *Journal of the Mechanics and Physics of Solids* 45 (5) (1997) 763–787.
- [11] V.C. Li, C. Wu, S. Wang, A. Ogawa, T. Saito, Interface tailoring for strain-hardening PVA-ECC, *ACI Materials Journal* 99 (5) (2002) 463–472.
- [12] J. Zhang, V.C. Li, Effect of inclination angle on fiber rupture load in fiber reinforced cementitious composites, *Composite Science and Technology* 62 (6) (2002) 775–781.
- [13] S. Wang, V.C. Li, Engineered cementitious composites with high-volume fly ash, *ACI Material Journal* 104 (3) (2007) 233–241.
- [14] Z. Lin, T. Kanda, V.C. Li, On interface property characterization and performance of fiber reinforced cementitious composites, *Journal of Concrete Science and Engineering*, RILEM 1 (3) (1999) 173–184.
- [15] B. Leng Investigation on High Ductile Fiber Reinforced Cement Composite, Master Thesis, Department of Civil Engineering, Tsinghua University, 2005.